# Transmission electron microscopy of coexisting low-tridymite polymorphs

J. R. ASHWORTH

School of Earth Sciences, University of Birmingham, P.O. Box 363, Birmingham B15 2TT

## Abstract

Three polymorphs of tridymite (MC, PO-10 and MX) have been examined by transmission electron microscopy (TEM), in crystals which also contain lamellae of cristobalite. MX is the least common, and is highly unstable in the electron beam. It occurs as small regions ($< 1$ $\mu m^2$) in PO-10 tridymite and at MC/PO-10 boundaries; these regions are interpreted as being strained. A consistent association between PO-10 and the cristobalite lamellae is attributed to the fact that PO-10 can more closely match the low-cristobalite structure than MC can, at boundaries parallel to the plane in which the crystal structures contain layers of $SiO_4$ tetrahedra. An analogous interpretation explains the observation that twin boundaries (associated with 60° or 120° rotation of the layer) are commonly parallel to the layer plane in PO-10 but at high angles to it in MC. Abundant lamellar features, parallel to the same plane in PO-10, are tentatively interpreted as representing twinning by reflection and 180° rotation, which may also account for $c^*$ streaking in diffraction patterns.

KEYWORDS: tridymite, polymorphism, twinning, transmission electron microscopy.

## Introduction

THE various low-temperature modifications of tridymite, reviewed by Wennemer and Thompson (1984), are derived from hexagonal high tridymite by different patterns of 'collapse' with lowering of symmetry. These high–low inversions are displacive (do not involve breaking of bonds), in contrast to the reconstructive (bond-breaking) transformation of tridymite to cristobalite, of which a TEM study has been presented (Ashworth, 1988). Low tridymites have been characterized by X-ray diffraction (XRD). It is common to find several of them within one crystal (Nukui and Flörke, 1987). As a contribution to understanding this diversity, the present work uses TEM to resolve small regions of such crystals.

The modifications encountered in this study are the three that are thought to be least unstable at ambient conditions, called MC, PO-10 and MX (Nukui and Flörke, 1984; Wennemer and Thompson, 1984). XRD studies have shown how the three lattices are related to hexagonal tridymite (Table 1). MC is a relatively well-defined phase; two structure determinations have been published (Kato and Nukui, 1976; Dollase and Baur, 1976), which were shown by Baur (1977) to be mutually consistent. PO-10, the structure of which was

investigated by Konnert and Appleman (1978), is one of a range of pseudo-orthorhombic tridymites PO-$n$, where $n$ is the multiplicity (relative to hexagonal tridymite) of the $c$ repeat (Wennemer and Thompson, 1984; Carpenter and Wennemer, 1985). In a TEM study of various synthetic tridymites, Carpenter and Wennemer (1985) identified MC and PO-$n$ ($n = 3$, 4, 5, and 6); they also defined a 'pseudohexagonal' tridymite which may be the same as MX, though they were unable to confirm subtle details which would be predicted from the XRD results of Hoffmann et al. (1983).

In tridymite (and cristobalite), the structure can be visualized in terms of layers of $SiO_4$ tetrahedra. These are parallel to the (0001) plane of high tridymite, which will be called the layer plane. The published structure determinations for MC and PO-10, together with work in progress on MX (Hoffmann, pers. comm.), indicate distinct styles of 'collapse' within the layer plane. Thus, the three modifications can be regarded as true polymorphs of tridymite, rather than polytypes (alternative sequence of stacking of layers). On the other hand, the existence of various values of $n$ in PO-$n$ suggests the possibility of a kind of (displacive) stacking disorder. This should not be confused with reconstructive stacking disorder, in which the tridymite

contains intercalated slabs of the cristobalite structure (~ 1 unit cell thick). However, Nukui and Flörke (1987) consider that the latter type of disorder is also associated with the occurrence of PO rather than MC tridymite. Carpenter and Wennemer (1985) found streaking parallel to $c^*$ in PO electron-diffraction patterns, and (0001) features in images, both effects indicating defects of some kind; these were tentatively interpreted as intercalations of cristobalite.

Schneider and Flörke (1986) performed heating experiments on single crystals. Untreated tridymite was characterized as MC. Where the experiments produced some cristobalite, PO tridymite was also detected by XRD. This tridymite is called PsOrh-5 by Schneider and Flörke (1986), but it is PO-10 in the nomenclature used here (following Wennemer and Thompson, 1984). The present TEM study of similar material was undertaken particularly to locate PO tridymite in crystals containing broad (> 100 nm) slabs of cristobalite.

## Methods

The specimens were pieces of a used refractory brick, experimentally heated at 1545 °C for 1 hour, 4 hours and 6 hours by Dr H. Schneider (Forschungsinstitut der Feuerfest-Industrie, Bonn). The cristobalite produced in these specimens is described by Ashworth (1988). Material for TEM was prepared by ion-beam thinning from doubly-polished thin-sections. All low-tridymite polymorphs rapidly become degraded in the electron beam to a state resembling high tridymite (Fig. 1a; see also Carpenter and Wennemer, 1985). However, using high-voltage electron microscopy to retard the rate of beam damage, it has been possible to obtain much information prior to degradation. The instruments used were an AEI-Kratos EM7 operating at 1 MV, and a JEOL 4000FX operating at 400 kV. Electron diffraction

is used to identify polymorphs, to characterize twinning, and to assess disorder. Identification is based on the relations given in Table 1, with some additional complications in MX (described below). Compared with XRD, electron diffraction does not yield as accurate cell parameters, nor are intensities as easily interpretable (partly because of double diffraction). Its usefulness is that patterns are obtained from small areas by using an aperture ~ 1 $\mu$m in diameter, and in ion-beam thinned specimens large parts of a crystal can be sampled in this way. A disadvantage of these relatively bulky specimens is that they cannot be subjected to heating-cooling cycles in the electron beam to study high-low inversions *in situ*, as was done by Carpenter and Wennemer (1985) using tiny crushed fragments. Ion-beam thinning inevitably heats the specimens to ~ 100 °C, so they may have been cycled through temperatures of approximately 110 °C at which PO and MC invert to higher-temperature modifications (Nukui et al., 1978; Wennemer and Thompson, 1984). These inversions are usually reversible (Nukui et al., 1978; Carpenter and Wennemer, 1985; Hoffmann, pers. comm.), so the net effect should be minimal. Some MX, on the other hand, may be lost by irreversible annealing to PO (Hoffmann et al., 1983). In this respect, the present procedure may have the reverse effect to the procedure of Carpenter and Wennemer (1985) who, as they were aware, may have produced MX during crushing (by the stress-induced transformation from MC discussed by Hoffmann et al., 1983). A major advantage of the uncrushed specimens is that boundaries can be found. In addition to boundaries between polymorphs, twin boundaries are expected, because low tridymites are commonly twinned by rotations through multiples of 60° (pseudohexagonal twinning). The effects of such twinning in XRD of MC tridymite have been described in detail by Tagai et al. (1977). The orientations of boundaries will be shown to be relevant to the

Table 1. Some crystallographic properties of low-tridymite polymorphs

| | Unit-cell shape, centring | Derivation of lattice vectors from those of high tridymite | | | Source of information |
|---|---|---|---|---|---|
| | | a | b | c | |
| MC | monoclinic C | 2a+b+2c | b | -6a-3b | Kato and Nukui (1976) |
| PO-10 | pseudo-orthorhombic F | 2b | -4a-2b | 10c | Konnert and Appleman (1978) |
| MX | monoclinic C | b | -2a-b | c | Hoffmann et al. (1983) |

interpretation of polymorph distribution, specifically the PO/cristobalite association.

## Electron-diffraction characteristics of polymorphs

MC, PO and MX tridymite were identified in crystals showing partial transformation to cristobalite. In a specimen that had not been heated sufficiently to produce any cristobalite ('unreacted brick specimen' of Ashworth, 1988) only MC was found. MC has already been well characterized by electron diffraction (Carpenter and Wennemer, 1985, Fig. 5). In this section, attention is concentrated on the more problematic PO and MX modifications. As previously noted by Carpenter and Wennemer (1985), the most instructive zones are those corresponding to $\langle 1\bar{1}.0 \rangle$ of hexagonal tridymite (Fig. 1).

*PO tridymite.* In contrast to the material studied by Carpenter and Wennemer (1985), PO in the present specimens has rather consistent properties throughout. The reciprocal lattice shows characteristic superlattice reflections along all rows parallel to $c^*$ (Fig. 1b and c) which reduce the reciprocal-lattice repeat distance by a factor of five relative to hexagonal 0001. The two different patterns derived from hexagonal $\langle 1\bar{1}.0 \rangle$, one of which has an 'offset' of half the short repeat distance between alternate rows of reflections (Fig. 1b), must represent different orientations of a PO-10 reciprocal lattice with systematic absences due to centring. One orientation is related to the other by a rotation of 60° (or, indistinguishably, 120°) about $c$, i.e. by pseudohexagonal twinning. The present observations indicate an F-centred lattice, as found by Konnert and Appleman (1978), rather than $C$-centred as inferred by Carpenter and Wennemer (1985) in generally more disordered material. It is possible that apparent $C$-centring could arise from superimposition of two zones related by the pseudohexagonal twinning.

In some examples of the $h0l$ pattern of PO, reflections with $h+l \neq 4n$ are weak (Fig. 1c). However, in other observations of the same zone, this effect is less pronounced (compare Fig. 1c with Fig. 1d and e), and in no case are the weak reflections completely absent.

There is streaking parallel to $c^*$ in some PO patterns (Fig. 1e), but the discrete reflections remain sharp and undistorted. The polymorph is well-ordered PO-10, with little or no contribution from any PO-$n$ structure having $n \neq 10$.

*MX tridymite.* This is thought to be the first confirmation of MX by electron diffraction. It is rare in the present material, and its patterns are only seen together with PO, as illustrated in Fig. 1d and e which show two distinct MX zones related by 60° or 120° rotation, analogous to the two distinct PO-10 zones of Fig. 1b and c.

As described by Hoffmann *et al.* (1983), MX has two particularly distinctive features: (1) the zones corresponding to hexagonal $\langle 1\bar{1}.0 \rangle$ have non-orthogonal principal vectors ($c^*$ of MX is parallel to hexagonal $c^*$ but MX has no vector exactly parallel to hexagonal $11\bar{2}0$); and (2) MX has an incommensurate superstructure. These effects are most clearly seen by comparing the $h0l$ pattern of MX with the PO reflections that form rows (parallel to hexagonal $c^*$) in Fig. 1d. The non-orthogonal property of MX produces a row-parallel component in the displacement of the arrowed reflections from the adjacent PO reflections. Unlike the arrowed reflections, those of the type labelled A and B do not exactly form rows parallel to hexagonal $c^*$; they are incommensurate, and form pairs of satellites about the other (sub-cell) reflections. It is possible to estimate lattice parameters for MX, using the superimposed PO patterns for calibration and assuming that PO has the lattice parameters given by Konnert and Appleman (1978). Within the uncertainties expected in electron diffraction (approximately 1%), both the parameters of the sublattice and the positions of the satellite reflections agree with those reported by Hoffmann *et al.* (1983). In the other pattern derived from hexagonal $\langle 1\bar{1}.0 \rangle$, incommensuracy is less obvious but still discernible (Fig. 1e).

MX is found to be more sensitive to the electron beam than PO; the MX reflections usually disappear irreversibly within a few seconds, leaving the PO pattern only.

## Distribution of polymorphs

PO is found to be associated with the cristobalite, which is topotactically related to the tridymite in these specimens and occurs as broad (up to 2 $\mu$m) lamellae. Their boundaries are parallel to the layer plane and in strict lattice orientation with respect to the tridymite (Ashworth, 1988). Although all three tridymite polymorphs can be located within a few $\mu$m of this cristobalite, only PO was identified in direct contact with the lamellae.

The constant association of MX with PO in diffraction patterns from areas $\sim 1\ \mu\text{m}^2$ indicates that it forms small regions in PO. One interesting effect was noticed when sampling PO/MC boundaries in diffraction; in three cases, a pattern from MX was found in addition to the other two (Fig. 2 is an example). Here, the MX is associated not
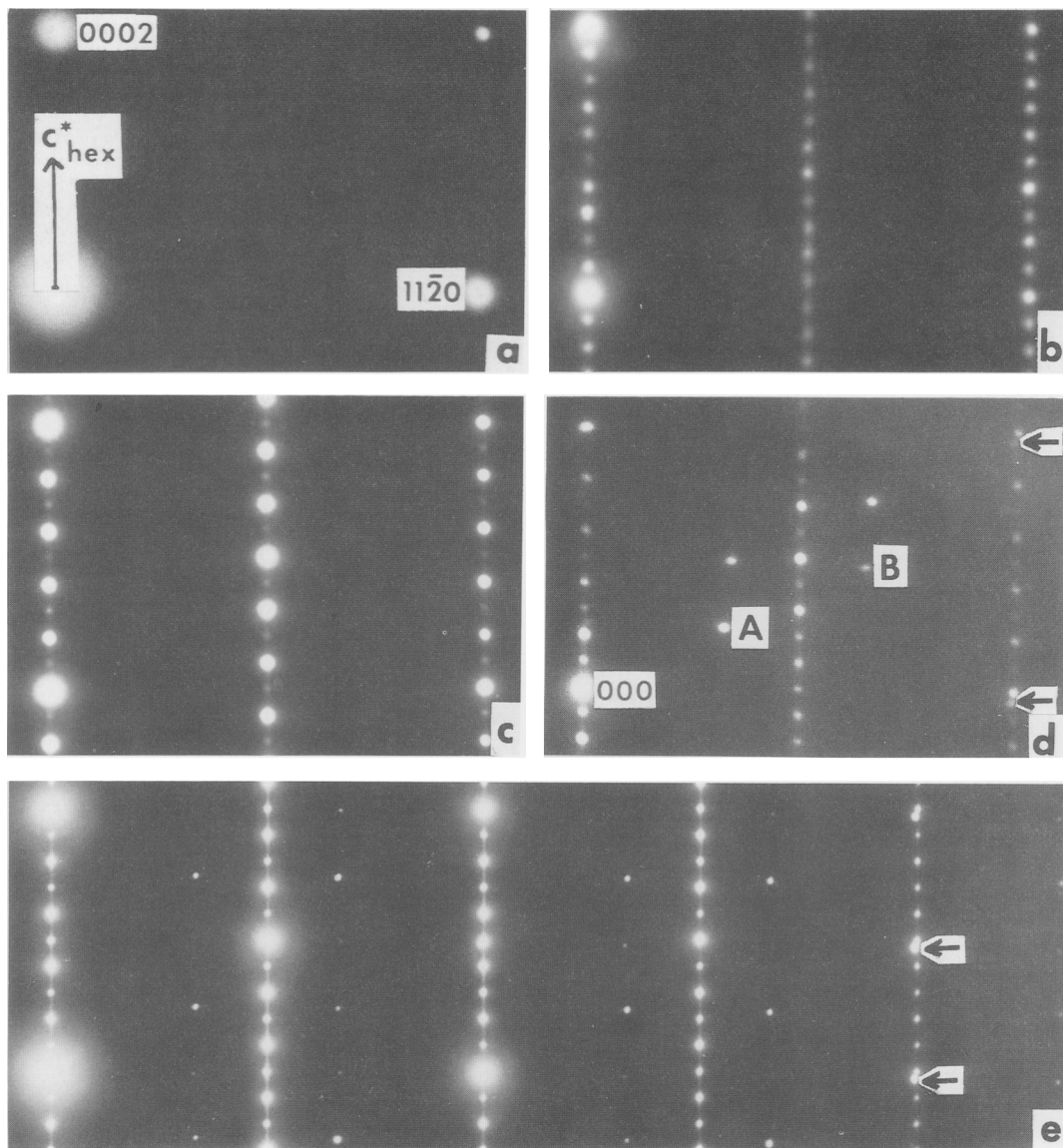
FIG. 1. Electron diffraction patterns corresponding to the ⟨1$\bar{1}$.0⟩ zone of high (hexagonal) tridymite. (a) Tridymite after long exposure to the beam (degraded tridymite). The pattern is like that of high tridymite, having systematic absences for $l \neq 2n$ due to a glide plane. (b) and (c) PO-10 tridymite: (b) 'with offset', zone [310] or [3$\bar{1}$0]. (c) 'without offset', zone [010]. (d) and (e) PO-10 [010], together with MX tridymite. The main (subcell) reflections of MX lie close to the PO rows. In (d) the MX zone is [010]; the subcell reflections (arrowed in the 20$l$ row) indicate monoclinic symmetry ($\beta \neq 90°$). The first-order and second-order satellite reflection of the 000 beam are labelled A and B respectively. In (e) the MX zone is [310]; subcell reflections of the $\bar{1}$3$l$ row are not resolved from PO reflections, but those of the $\bar{2}$6$l$ row are distinct (two of these MX reflections are arrowed).
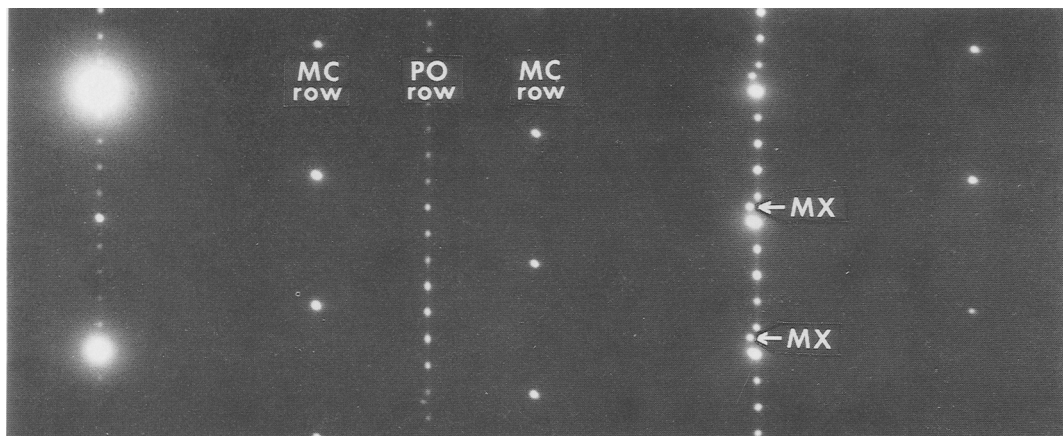
FIG. 2. Electron-diffraction pattern of PO, MC and MX tridymite, corresponding to $\langle 2\bar{1}.0 \rangle$ of hexagonal tridymite. MX gives reflections near a PO row, two of which are arrowed.

simply with PO but specifically with its boundary against MC.

### Boundaries within tridymite

Because of its scarcity and rapid transformation in the beam, MX could not be imaged. In the other two polymorphs, two kinds of boundary are obvious: pseudohexagonal twin boundaries (Fig. 3a and c) and PO/MC boundaries (Fig. 3b). Twin boundaries between the distinguishable orientations of PO (related by 60° or 120° rotation) are abundant. They are mostly oriented exactly parallel to the layer plane, but may have 'steps' at a high angle to it (Fig. 3a). They are very distinct from PO/MC boundaries (of which 4 were imaged) and twin boundaries in MC (6 imaged), both of which are curved and make high angles with the layer plane (Fig. 3b and c). There is evidence of strain adjacent to PO/MC boundaries (Fig. 3b).

An additional feature of PO comprises ubiquitous lamellae parallel to the layer plane. These are not found in MC. They give weak contrast in images. They are present in Fig. 3b, and in Fig. 3a where they are very faint and thus distinguishable from the single, pseudohexagonal twin boundary. They are shown without other features in Fig. 4a, which typifies their weak contrast. (It was not possible to assess contrast as a function of diffraction vector by exciting different reflections singly, because the short $c^*$ spacing makes it inevitable that several reflections are simultaneously excited). These lamellar features disappear irreversibly as the PO tridymite degrades in the beam (as the diffraction pattern loses the superlattice reflections); this implies that they are related to the low-

tridymite superlattice and are not reconstructive stacking faults. They are distinct from much rarer lamellae, which (like broad cristobalite lamellae) persist after degradation of the tridymite and can be brought into strong contrast (Fig. 4b); the latter probably are due to reconstructive faults (i.e. cristobalite intercalations).

### Discussion

*Distribution of polymorphs.* Since the formation of MX tridymite is known to be favoured by stress, it is likely that the small MX areas in PO are areas of stress concentration. This is consistent with the occurrence of MX at PO/MC boundaries, for which there is independent evidence of strain (Fig. 3b). The rapid disappearance of MX during observations is likely to be a thermal annealing effect (cf. Hoffmann *et al.*, 1983), due to mild heating by the beam. Carpenter and Wennemer (1985) also transformed 'pseudohexagonal' tridymite irreversibly in the electron beam; deliberately applying strong heating, they produced a higher-temperature polymorph which then inverted to PO on cooling.

The major spatial association observed is between PO tridymite and lamellar cristobalite. This supports the inference, from the data of Schneider and Flörke (1986), that partial topotactic transformation to cristobalite is followed, during cooling, by inversion of the tridymite to the PO polymorph. The results indicate that coherent (or nearly coherent) cristobalite/tridymite boundaries, parallel to (0001) of the high tridymite, induce formation of PO. This can be explained by comparing the crystal structures of low tridymites (Dollase

FIG. 4. Lamellar features parallel to the layer plane in tridymite. The scale is the same for both photomicrographs. (a) Typical, subdued contrast in PO tridymite. (b) Isolated lamellae in degraded tridymite, in strong contrast with the $h0\bar{h}0$ row of reflections strongly excited.
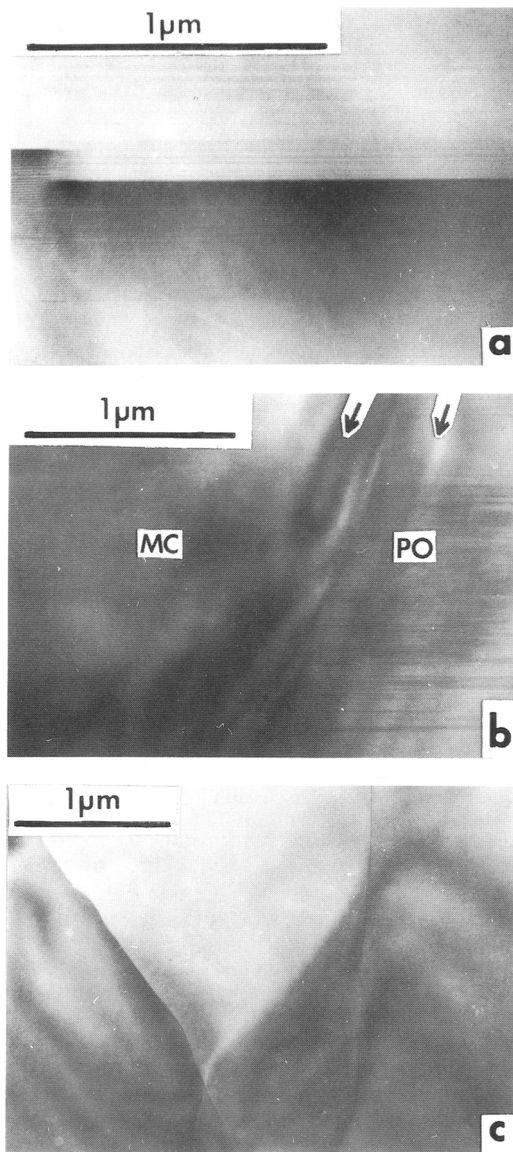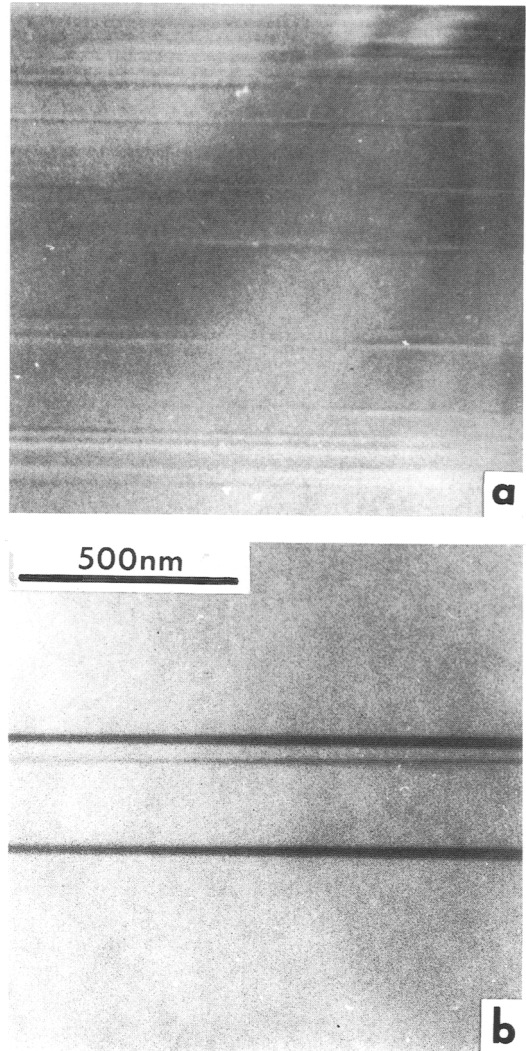
FIG. 3. TEM photomicrographs showing boundaries within tridymite. In all cases, the layer plane is parallel to the long edges of the photograph. (a) Pseudohexagonal twin boundary in PO tridymite. (b) Boundary between PO and MC. Arrows locate fringes approximately parallel to the boundary, due to localized strain on either side of it. (c) Pseudohexagonal twin boundaries in MC.

and Baur, 1976; Konnert and Appleman, 1978) with the only known low-cristobalite structure (Dollase, 1965), as follows.

The observed boundary plane is parallel to the layer plane, within which the $SiO_4$ tetrahedra share oxygen atoms so as to form rings (Fig. 5). In both high tridymite and high cristobalite, the rings are nearly perfectly hexagonal in shape. In the 'collapsed' structure of low cristobalite, all rings are the same shape ('oval') (Fig. 5a), whereas in MC tridymite, one row of oval rings alternates with two rows of ditrigonal rings. Both structures have straight rows of up-pointing and down-pointing tetrahedral apices, but they have different spacings between rows (Fig. 5). The sharing of
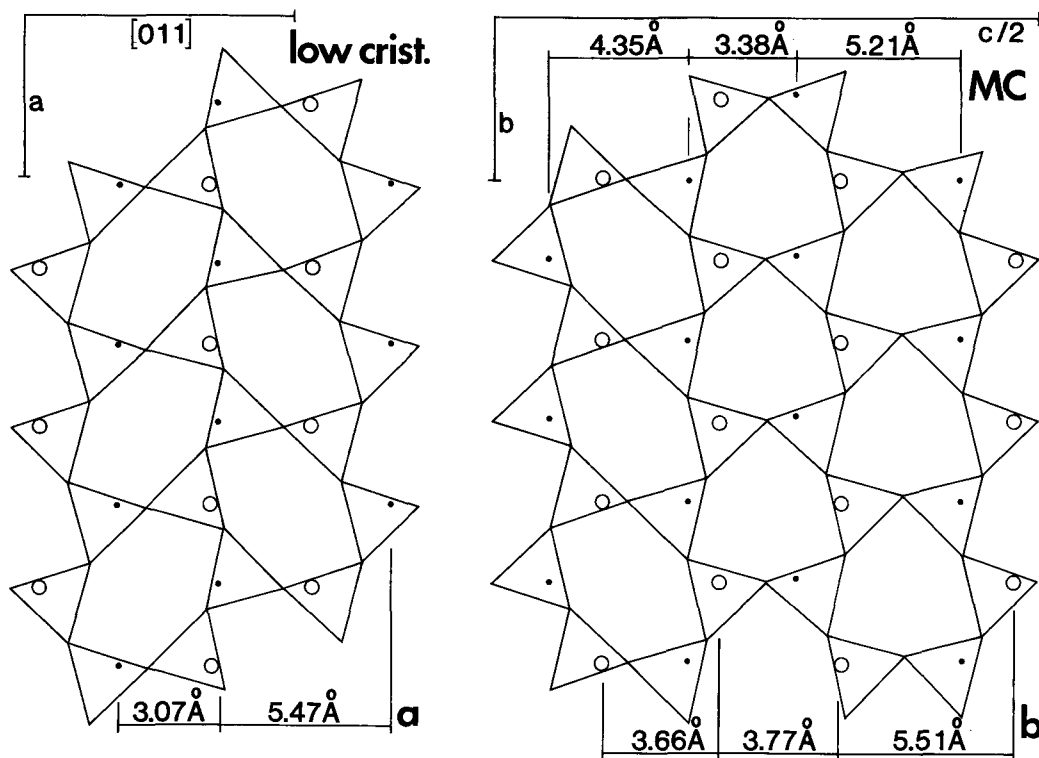
FIG. 5. The SiO$_4$ tetrahedra in a representative part of a layer (projected on to the layer plane) in the crystal structures of low cristobalite and MC tridymite. Dots indicate up-pointing apices of tetrahedra, circles down-pointing apices. (*a*) Low cristobalite, plotted from the atomic co-ordinates of Dollase (1965). (*b*) MC tridymite, from the atomic co-ordinates of Dollase and Baur (1976) but with axes labelled according to the setting of Kato and Nukui (1976).

these apices (out-of-layer oxygen atoms) at a junction between the different layers would involve considerable strain. In contrast to MC, the PO-10 structure of Konnert and Appleman (1978) comprises rows of parallel oval rings, very like those in low cristobalite, so a relatively good fit is possible (Fig. 6*a*). Rows of well-matched apices (mismatch < 0.1 Å) alternate with less well-matched rows (mismatch 0.9–1.0 Å). Despite this seemingly poor match for half the apices, the fit is much better than for a low-cristobalite/MC boundary, in which only one-third of apices could be well-matched and mismatches > 1 Å could not be avoided. Thus, the distortions required to join low tridymite to low cristobalite, with a boundary parallel to the layer plane, are less if the tridymite is PO than if it is MC. It is inferred that the coexistence with cristobalite at a (0001) boundary is the constraint causing the tridymite locally to invert to PO. After the boundary had formed between high tridymite and high cristobalite, the

inversion of the cristobalite to its low polymorph during cooling through about 270 °C (Wennemer and Thompson, 1984) controlled the subsequent behaviour of adjacent tridymite.

*Boundaries within tridymite.* Because of the similarity between PO and low cristobalite, the mismatches when a PO layer is superimposed on MC are similar to those discussed above for low cristobalite on MC. Also, in MC twinned by 60° or 120° rotation, there would be complex mismatches at a layer-plane boundary, with the straight rows of apices overlaying zig-zag rows in the rotated structure. Thus it is hardly surprising that neither PO/MC boundaries, nor twin boundaries associated with 60° or 120° rotation in MC, are parallel to the layer plane. Unlike the MC, the PO-10 structure contains adjacent layers in which the rows of oval rings run in different directions, 60° apart. A similar boundary between twin-related layers (Fig. 6*b*) has mismatches comparable
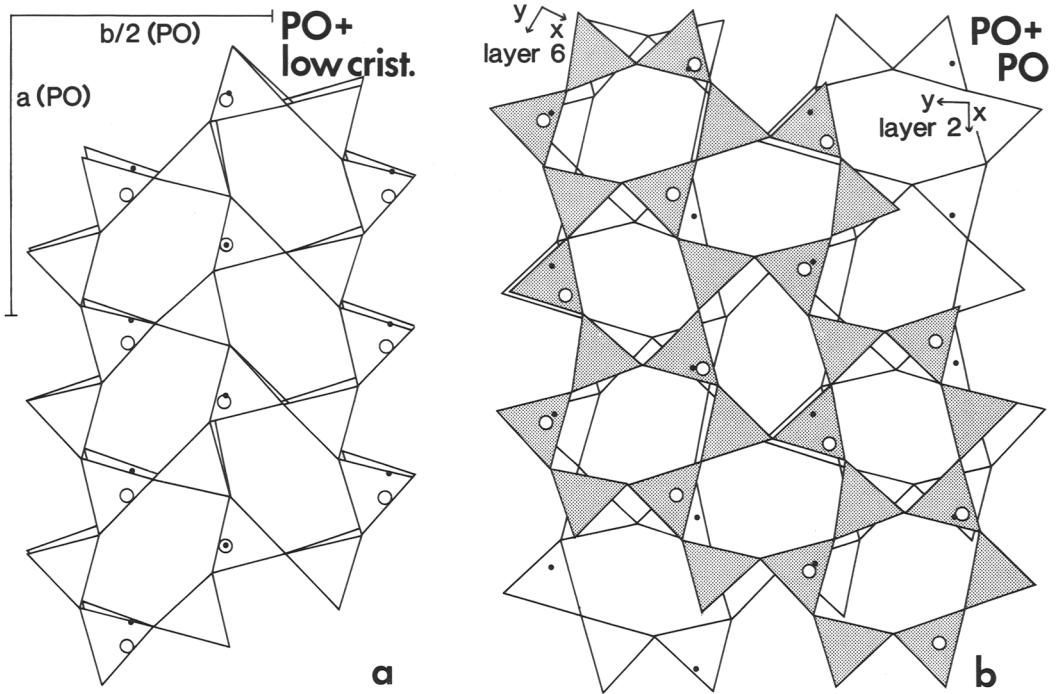
FIG. 6. Models of boundaries represented by superimposed layers of crystal structure. Mismatches between up-pointing apices of the lower layer (dots) and down-pointing apices of the upper layer (circles) give a measure of the distortions required in the structure near a real boundary, where these apices must be coincident. PO-10 layers are plotted from the atomic co-ordinates of Konnert and Appleman (1978). (*a*) Layer 5 of the PO-10 structure over the low-cristobalite layer of Fig. 5*a*. (*b*) Layer 6 (stippled) over layer 2 of PO-10 with a rotation of 60° between their crystallographic axes, to represent twinning.

to those in Fig. 6*a*, and serves as a model for the layer-parallel pseudohexagonal twin boundaries observed in PO.

Remaining to be interpreted are the abundant layer-parallel features in PO which give relatively weak contrast (Fig. 4*a*). A tentative interpretation can be offered by reference to the XRD study of Konnert and Appleman (1978), who inferred that their PO crystal was pervasively twinned in such a way as to relate the X-ray intensities of the reflections $hkl$, $hk\bar{l}$, $\bar{h}kl$ and $\bar{h}k\bar{l}$. This requires mirror operation(s) and/or 180° rotation(s). The abundant features may possibly represent such twinning, because the pseudosymmetry in the structure of Konnert and Appleman (1978) implies very close matches at such twin boundaries parallel to the layer plane (all mismatches ≤ 0.3 Å in model boundaries). Involving less distortion than the 60° or 120° rotation boundaries, the reflection or 180° rotation boundaries are expected to occur more commonly, and can explain not only the features in images but also the streaking parallel to $c^*$ in some electron-diffraction patterns (as

being due to numerous twin lamellae of various, small widths). There may be other defects present. The variation in relative intensities in the $h0l$ pattern (Fig. 1*c*, *d* and *e*) is probably not an artefact of double diffraction, since Hoffmann (pers. comm.) has found the same effect in XRD; he suggests that it may be due to defects in an underlying structure that differs from the one proposed by Konnert and Appleman (1978) and, if perfect, would give systematic absences due to a glide plane in this zone.

Whatever the precise origin of the pervasive lamellar effect, the versatility of the PO structure in forming layer-parallel boundaries is clearly shown by its pseudohexagonal twinning. The existence of the layer-parallel, 60° or 120° rotation boundaries supports the interpretation of the PO/low-cristobalite coexistence, because modelling these twin boundaries reveals mismatches slightly greater than in the model for the PO/low-cristobalite boundary. The implication is that distortions are possible, near the real boundary, to accommodate the mismatches (of approximately 1 Å relative to

perfect layer junctions). Bourret *et al.* (1986) discuss mismatches of comparable size at twin boundaries in another silica mineral (coesite).

In summary, the occurrence of MX and PO rather than MC in parts of the specimens is attributable to special factors. In the case of MX these are probably small-scale strains, which are due to the previous history of thermal cycling, and can be relieved by annealing in the electron beam. PO is formed as a result of interface effects at junctions with lamellar cristobalite. From the latter finding, it follows that reconstructive stacking disorder should strongly constrain tridymite to adopt the PO structure at low temperature. On the other hand, this work shows that such disorder is not a necessary precondition for the PO/cristobalite association; the present tridymite is not disordered in this sense. The origin of the pervasive lamellar features is displacive. Their association with some $c^*$ streaking in diffraction indicates that this origin should be considered, as an alternative to reconstructive stacking disorder, for $c^*$ streaks in diffraction patterns from other specimens.

## Acknowledgements

## References

Ashworth, J. R. (1988) Transformation mechanisms of tridymite to cristobalite studied by transmission electron microscopy. *Phys. Chem. Minerals*, **15**, 246–51.

Baur, W. H. (1977) Silicon–oxygen bond lengths, bridging angles Si–O–Si and synthetic low tridymite. *Acta Crystallogr.* **B33**, 2615–19.

Bourret, A., Hinze, E., and Hochheimer, H. D. (1986) Twin structure in coesite studied by high resolution electron microscopy. *Phys. Chem. Minerals*, **13**, 206–12.

Carpenter, M. A., and Wennemer, M. (1985) Characterization of synthetic tridymites by transmission electron microscopy. *Am. Mineral.* **70**, 517–28.

Dollase, W. A. (1965) Reinvestigation of the structure of low cristobalite. *Z. Kristallogr.* **121**, 369–77.

——and Baur, W. H. (1976) The superstructure of meteoritic low tridymite solved by computer simulation. *Am. Mineral.* **61**, 971–8.

Hoffmann, W., Kockmeyer, M., Löns, J., and Vach, Chr. (1983) The transformation of monoclinic low-tridymite MC to a phase with an incommensurate superstructure. *Fortschr. Mineral.* **61**, Beiheft 1, 96–8.

Kato, K., and Nukui, A. (1976) Die Kristallstruktur des monoklinen Tief-Tridymits. *Acta Crystallogr.* **B32**, 2486–91.

Konnert, J. H., and Appleman, D. E. (1978) The crystal structure of low tridymite. Ibid. **B34**, 391–403.

Nukui, A., and Flörke, O. W. (1984) Coexistence of tridymite polymorphs and cristobalite in tridymite crystals. Ibid. **A40**, C-257.

————(1987) Three tridymite structural modifications and cristobalite intergrown in one crystal. *Am. Mineral.* **72**, 167–9.

——Nakazawa, H., and Akao, M. (1978) Thermal changes in monoclinic tridymite. Ibid. **63**, 1252–9.

Schneider, H., and Flörke, O. W. (1986) High-temperature transformation of tridymite single crystals to cristobalite. *Z. Kristallogr.* **175**, 165–76.

Tagai, T., Sadanaga, R., Takéuchi, Y., and Takeda, H. (1977) Twinning of tridymite from the Steinbach meteorite. *Mineral. J.* **8**, 382–98.

Wennemer, M., and Thompson, A. B. (1984) Tridymite polymorphs and polytypes. *Schweiz. Mineral. Petrogr. Mitt.* **64**, 335–53.